

TABLE OF CONTENTS

	Page
ACKNOWLEDGEMENTS	iii
ABSTRACT (ENGLISH)	v
ABSTRACT (THAI)	viii
LIST OF TABLES	xiv
LIST OF ILLUSTRATIONS	xv
ABBREVIATIONS	xxi
CHAPTER 1: INTRODUCTION AND OBJECTIVES	1
1.1 Introduction	1
1.2 Objectives	3
CHAPTER 2: THEORY AND LITERATURE SURVEY	4
2.1 Piezoelectricity	4
2.2 Perovskites	10
2.3 Single Phase Piezoelectric Materials	11
2.3.1 Ceramic Piezoelectric Materials	11
2.3.1.1 Lead Zirconate Titanate	12
2.3.1.2 Lead Titanate	19
2.3.1.3 Lead Metaniobate	20
2.3.2 Polymer Piezoelectric Materials	22
2.3.2.1 Polyvinylidene Fluoride (PVDF)	22
2.3.2.2 P(VDF-TrFE) Copolymer	23
2.4 Matrix Phase : Thermoset Resin	25
2.4.1 Epoxy	25

	Page
2.5. Piezoelectric Ceramic-Polymer Composites	27
2.5.1 Phase connectivity	30
2.5.2 Piezocomposites with 0-3 Connectivity	33
2.5.3 Piezocomposites with 1-3 Connectivity	39
2.6 Piezoelectric Ceramic-Polymer Applications	42
2.6.1 Hydrophone Applications	43
2.6.2 Biomedical Imaging Applications	44
2.7 Composite Processing and Fabrication	47
2.8 Summary	50
CHAPTER 3 EXPERIMENTAL METHODS AND PROCEDURES	51
3.1 Fabrication of PZT Powders	51
3.1.1 Preparation of PZT powder by spray drying technique	52
3.1.2 Preparation of PZT powder by mixed oxide method	53
3.1.3 Preparation of PZT powder by modified method	54
3.2 Processing of 0-3 ceramic-polymer composites	57
3.3 Characterization and Measurement Methods	61
3.3.1 Thermal Analysis	61
3.3.2 Particle Size Analysis of PZT powder	61
3.3.3 X-Ray Diffraction Analysis	61

	Page
3.3.4 Scanning Electron Microscopy (SEM)	62
3.3.5 Transmission Electron Microscopy (TEM)	62
3.3.6 Energy Dispersive Spectroscopy	63
3.4 Property Measurement of the Composites	64
3.4.1 Density Measurement	64
3.4.2 Polarization of the Composites	65
3.4.3 Dielectric Properties	66
3.4.4 Piezoelectric Properties	66
3.4.5 Acoustic Impedance	68
CHAPTER 4 RESULTS AND DISCUSSIONS	70
4.1 Characterization of PZT sample made by spray dry technique	70
4.1.1 Thermal Analysis of PZT sprayed powder	70
4.1.2 X-ray Diffraction Results	72
4.1.2.1 Spray dry powder	72
4.1.2.2 Spray dry ceramics	75
4.1.3 Determination of the Particle Size	77
4.1.4 Examination of sprayed PZT powder by SEM and TEM	81
4.2 Characterization of PZT sampler made by conventional mixed oxide method	95
4.2.1 Phase formation of PZT powder	95

	Page
4.2.2 Investigation of particle size distribution of PZT mixed oxide powder	98
4.2.3 Examination of PZT mixed powder by SEM	101
4.3 Characterization of modified PZT sample	111
4.3.1 Phase transformation of modified PZT ceramics	111
4.3.2 Microstructure of modified PZT	113
4.4 Physical properties of PZT ceramics	120
4.5 Dielectric and piezoelectric properties of PZT ceramics	122
4.6 Properties of Piezoceramic-Polymer Composites	126
4.6.1 Physical properties	126
4.6.2 Dielectric Properties and Piezoelectric Properties	128
4.7 Scanning Electron Micrographs of Composites	130
CHAPTER 5: CONCLUSIONS	135
5.1 Powder Processing and Characterization	135
5.2 Composite Processing and Characterization	136
5.3 Suggestion for Future Work	137
REFERENCES	138
APPENDIX	148
VITA	174

LIST OF TABLES

Table		Page
2.1	Electromechanical properties of ceramic piezoelectric materials.	21
2.2	Optimum transducer material properties for low and high frequency applications.	46
4.1	JCPDS Powder Diffraction File of PZT powder.	73
4.2	The relationship of physical properties and sintering temperature of PZT ceramics	121
4.3	Dielectric and piezoelectric properties of the PZT ceramics produced from the spray dried granules.	123
4.4.	Dielectric and Piezoelectric properties of the PZT ceramics produced from the mixed oxide powder.	124
4.5.	Piezoelectric, dielectric and physical properties of the PZT ceramics produced from the mixed oxide powder.	125
4.6	Physical and mechanical properties of the PZT/polymer composites PZT(m), PZT(sp) = powders obtained from mixed oxide method and spray drying techniques, respectively.	127
4.7	Dielectric and piezoelectric properties of the PZT/polymer composites compared with those of previous work.	129

LIST OF ILLUSTRATIONS

Figure		Page
2.1	Piezoelectric effects in ferroelectric ceramics [12].	5
2.2	Schematic representation of piezoelectric response under the electric field E.	8
2.3	The unit cell and ABO_3 perovskite structure of PZT [12].	10
2.4	The phase diagram of $Pb(Zr_{1-x}Ti_x)O_3$ [15].	13
2.5	The epoxide group of epoxy matrix.	25
2.6	Ten different connectivity patterns of diphasic Materials [67].	31
2.7	Schematic diagram of various piezoelectric ceramic-polymer composites.	32
2.8	Schematic diagram of 0-3 ceramic-polymer composite.	33
2.9	(a) 1-3 piezoceramic-polymer composite. (b) Fabrication the rod array for a 1-3 piezoceramic-polymer composite by injection moulding.	49
3.1	Schematic of preparation of PZT samples by using spray drying technique.	55
3.2	Schematic of preparation of PZT samples by using mixed oxide method.	56
3.3	Schematic of the equipment to prepare 0-3 piezoceramic/epoxy resin composites. The PZT/powders and resin were filled in a syringe with a filter underneath. The syringe was plugged in a flask partly filled with water. Suction was carried out through an air pump.	59

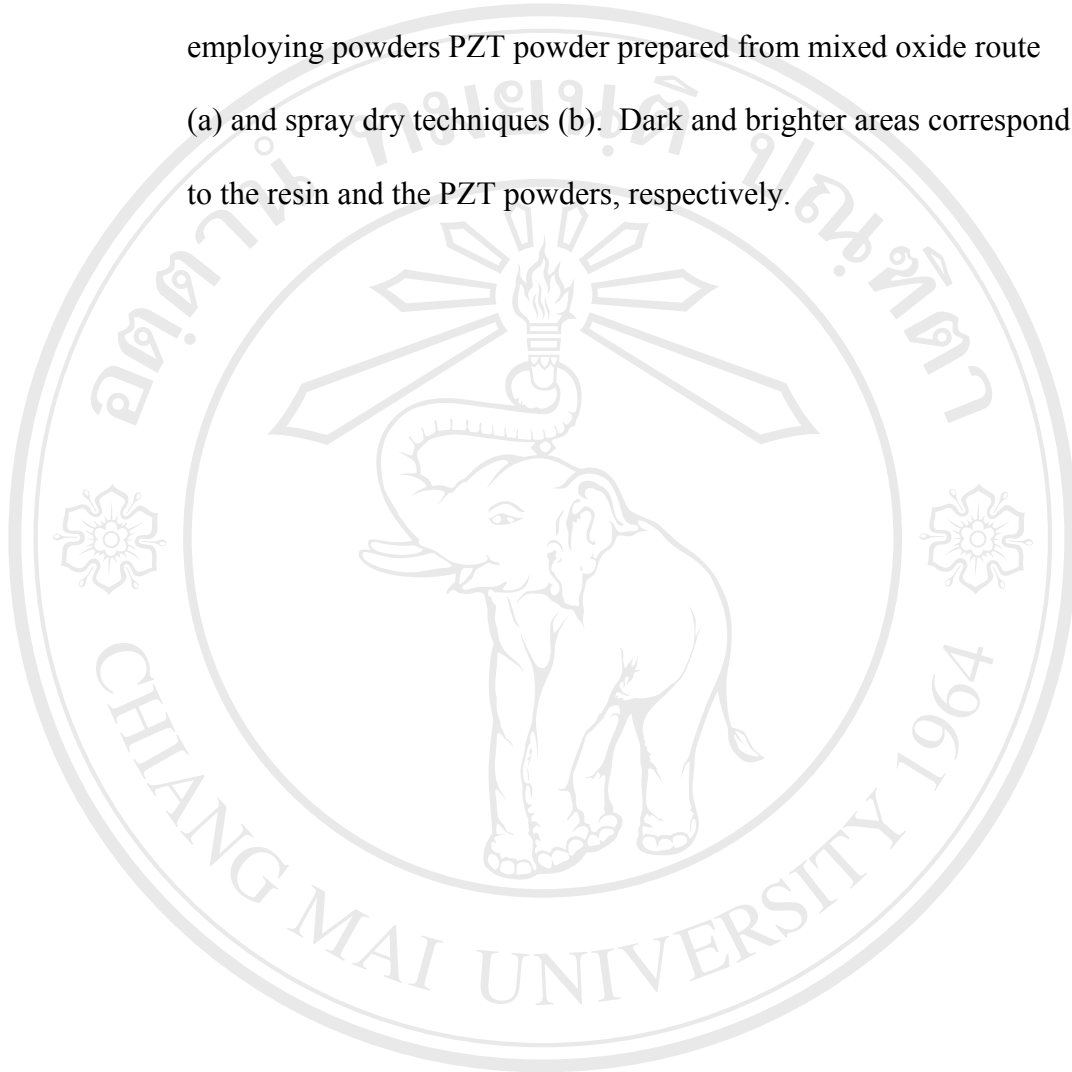
Figure	Page
3.4 Schematic of photograph of (0-3) and (1-3) combined piezocomposite sample where polymer matrix = epoxy resin filled in the spaces to form the 1-3 connectivity with 0-3 ceramic/polymer rods (0.35×0.35 mm.)	60
3.5 The poling apparatus.	65
3.6 Equivalent circuit of the piezoelectric Material [15].	67
3.7 The circuit diagram for measuring of f_r and f_a .	67
3.8 Diagram of the apparatus for echo shift measurement.	69
4.1 DTA and TG thermograms of the spray dried granules.	71
4.2 XRD patterns of PZT powder made by spray dry technique calcined at different temperature.	74
4.3 XRD patterns of sprayed PZT ceramics sintered with various temperatures.	76
4.4 Particle size distribution of PZT sprayed powder calcined at (a) 500 °C and (b) 600 °C.	78
4.5 Particle size distribution of PZT sprayed powder calcined at (a) 700 °C and (b) 800 °C.	79
4.6 Particle size distribution of PZT sprayed powder calcined at 850 °C	80
4.7 SEM micrographs of sprayed powder (a) uncalcined and (b) calcined at 500 °C	83
4.8 SEM micrographs of sprayed powder calcined at (a) 600 °C and (b) 700 °C.	84
4.9 SEM micrographs of sprayed powder calcined at (a) 800 °C and (b) 850 °C.	85

Figure	Page
4.10 TED (a) and TEM (b) micrographs of selected area of PZT powder.	86
4.11 EDS spectrum of corresponding PZT powders.	87
4.12 The dark field image of PZT ceramics prepared from sprayed powder.	87
4.13 The bright field image of PZT ceramics prepared from sprayed powder	88
4.14 The bright field image of PZT ceramics prepared from sprayed powder with different angle.	88
4.15 SEM micrographs of as sintered surface of PZT ceramics fabricated from spray dried granules sintered at (a) 900 °C and (b) 1000 °C.	89
4.16 SEM micrographs of as sintered surface of PZT ceramics fabricated from spray dried granules sintered at (a) 1100 °C and (b) 1200 °C.	90
4.17 SEM micrographs of as sintered surface of PZT ceramics fabricated from spray dried granules sintered at (a) 1230 °C and (b) 1250 °C.	91
4.18 SEM micrographs of fracture surface of PZT ceramics fabricated from spray dried granules sintered at (a) 900 °C and (b) 1000 °C.	92
4.19 SEM micrographs of fracture surface of PZT ceramics fabricated from spray dried granules sintered at (a) 1100 °C and (b) 1200 °C.	93
4.20 SEM micrographs of fracture surface sprayed of PZT ceramics fabricated from spray dried granules sintered (a) 1230 °C and (b) 1250 °C.	94
4.21 XRD patterns of PZT mixed powder calcined with several temperatures. (* is the unreacted ZrO ₂)	96
4.22 XRD patterns of PZT mixed sample sintered with several temperatures.	97

Figure	Page
4.23 The particle size distribution of mixed oxide PZT powder calcined at temperature 500 °C.	98
4.24 The particle size distribution of mixed oxide PZT powder calcined at temperature (a) 600 °C and (b) 700 °C	99
4.25 Particle size distribution of mixed oxide PZT powder calcined at temperature (a) 800 °C and (b) 850 °C.	100
4.26 SEM micrographs of mixed oxide powder (a) uncalcined and (b) calcined at 500 °C.	102
4.27 SEM micrographs of mixed oxide powder calcined at (a) 600 °C and (b) 700 °C.	103
4.28 SEM micrographs of mixed oxide d powder calcined at (a) 800 °C and (b) 850 °C.	104
4.29 SEM micrographs of as sintered surface of mixed oxide ceramic sintered at (a) 900 °C and (b) 1000 °C.	105
4.30 SEM micrographs of as sintered surface of mixed oxide ceramic sintered at (a) 1100 °C and (b) 1200 °C.	106
4.31 SEM micrographs of as sintered surface of mixed oxide ceramic sintered at (a) 1230 °C and (b) 1250 °C.	107
4.32 SEM micrographs of fracture surface of mixed oxide ceramic sintered at (a) 900 °C and (b) 1000 °C.	108
4.33 SEM micrographs of fracture surface of mixed oxide ceramic sintered at (a) 1100 °C and (b) 1200 °C.	109

Figure	Page
4.34 SEM micrographs of fracture surface of mixed oxide ceramic sintered at (a) 1230 °C and (b) 1250 °C.	110
4.35 XRD patterns of PZT modified ceramics sintered at several temperatures.	112
4.36 SEM micrographs of as sintered surface of modified ceramics sintered at (a) 900 °C and (b) 1000 °C.	114
4.37 SEM micrographs of as sintered surface of modified ceramics sintered at (a) 1100 °C and (b) 1200 °C.	115
4.38 SEM micrographs of as sintered surface of modified ceramics sintered at (a) 1230 °C and (b) 1250 °C.	116
4.39 SEM micrographs of fracture surface of modified ceramics sintered at (a) 900 °C and (b) 1000 °C.	117
4.40 SEM micrographs of fracture surface of modified ceramics sintered at (a) 1100 °C and (b) 1200 °C.	118
4.41 SEM micrographs of fracture surface of modified ceramics sintered at (a) 1230 °C and (b) 1250 °C.	119
4.42 Top view photograph of the composite.	131
4.43 The typical SEM micrographs of top view of PZT/epoxy resin composites.	132
4.44 SEM micrographs of PZT/epoxy resin which PZT composites employing powders prepared from mixed oxide route (a) and spray dry techniques (b).	133

Figure		Page
4.45	SEM micrographs of cross section of PZT/epoxy resin composites employing powders PZT powder prepared from mixed oxide route (a) and spray dry techniques (b). Dark and brighter areas correspond to the resin and the PZT powders, respectively.	134



ลิขสิทธิ์มหาวิทยาลัยเชียงใหม่
Copyright © by Chiang Mai University
All rights reserved

ABBREVIATIONS

A	area
C	capacitance
c_L	longitudinal velocity
c/a	tetragonality
d	interplanar spacing
d_h	hydrostatic charge coefficient
d_{ij}	piezoelectric charge coefficient
d_{33}	piezoelectric charge coefficient
d_{hg}	hydrophone figure of merit
E_i	electric field
f_s	series resonance frequency
f_n	frequency when maximum impedance
f_r	resonance frequency
f_a	antiresonance frequency
g_h	hydrostatic voltage coefficient
g_{ij}	piezoelectric voltage coefficient
g_{33}	piezoelectric voltage coefficient
K	Bulk modulus
K_α	radiation of K series
k_p	planar coupling coefficient
k_t	thickness coupling coefficient
L	column length

P_i	electrical polarization
PZT	Lead Zirconate Titanate
PVDF	Polyvinylidene Fluoride
Q_m	mechanical quality factor
R_e	resistive component
R_1	resistance of the series branch
S	reciprocal space vector
SEM	Scanning Electron Microscopy
ΔT	time difference
$\tan\delta$	dissipation factor
t	thickness
Vol%	volume percentage fraction
W_d	dry ewight
W_w	wet weight
Z	acoustic impedance
ϵ_r	relative permittivity or dielectric constant
ϵ_0	permittivity of free space
ϵ_{ij}	mechanical strain
σ_j	mechanical stress
θ	Bragg's angle